ELNP SPbU

Educational Laboratory of Nuclear Processes

Saint Petersburg State University

Silicon Pixel Detectors for Digital Tracking Calorimetry

Vitalii Petrov*, Vladimir Zherebchevsky, Valery Kondratiev, Nicolay Maltsev

St. Petersburg State University

*vitalii17@bk.ru

International School of Subnuclear Physics
Erice, Italy

20.06.2024

Hadron therapy

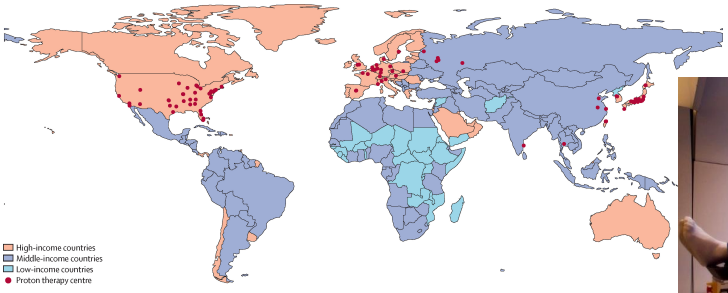

121 currently operating proton therapy centers in the world. Carbon therapy is available at 14 centers.
Lancet Oncol. 24 (2023) e245

Proton therapy centre in St. Petersburg.
ldc.ru

Hadron therapy

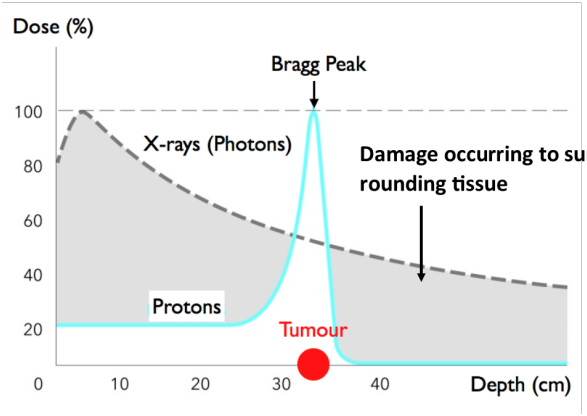

Depth distribution of energy losses for photons and protons.
https://www.avoplc.com/en-gb/LIGHT/The-Potential-of-Proton-Therapy

- The main advantage of proton beams is the mechanism of energy losses, which have maximum at the end of the proton path (Bragg curve).
- A large dose can be delivered precisely to the tumor region. The side effects on healthy tissue are minimal.

Hadron therapy

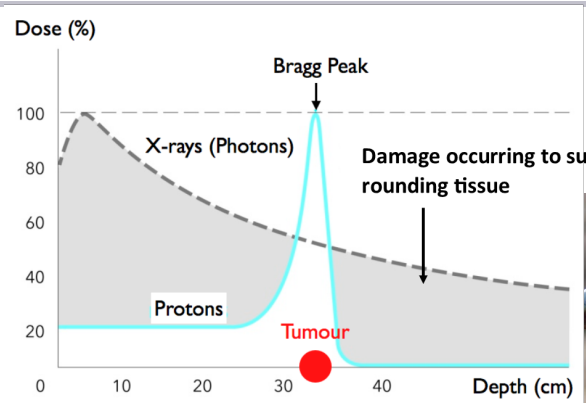

Depth distribution of energy losses for photons and protons.

https://www.avoplc.com/en-gb/LIGHT/The-Potential-of-Proton-Therapy

Analogy: a bullet cause more damage on exit.

Hadron therapy

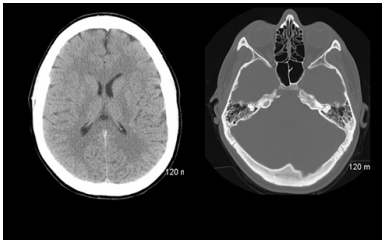

X-ray tomogram: grayscale display units of radiation attenuation (Hounsfield scale).

- To date, planning for patients of proton therapy is mostly done using X-ray CT.
- The X-ray CT data are recalculated into the stopping power in the medium for protons.
- The difference in the interaction of p and X-ray leads to uncertainties.

As a result: the error is about 2-3% (4-6 mm at a depth of 20 cm) for the estimated distances of protons.

Hadron therapy

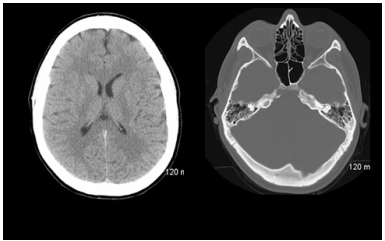

X-ray tomogram: grayscale display units of radiation attenuation (Hounsfield scale).

- To date, planning for patients of proton therapy is mostly done using X-ray CT.
- The X-ray CT data are recalculated into the stopping power in the medium for protons.
- The difference in the interaction of p and X-ray leads to uncertainties.

As a result: the error is about 2-3% (4-6 mm at a depth of 20 cm) for the estimated distances of protons.

Solution: Use same particles for diagnostic and therapy - Proton Computed Tomography

Digital tracking calorimetry

Digital tracking calorimeter prototype by Bergen pCT collaboration.

J. Alme et al, Front. Phys. Sec. Med. Phys. and Imag. 2020; 8, 20.

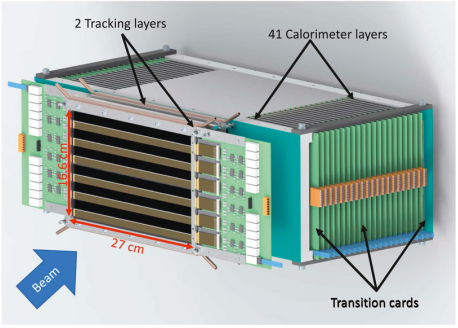

The track calorimeter consists of layers of pixel detectors and aluminium absorbers.

Digital tracking calorimetry

Digital tracking calorimeter prototype by Bergen pCT collaboration.

J. Alme et al, Front. Phys. Sec. Med. Phys. and Imag. 2020; 8, 20.

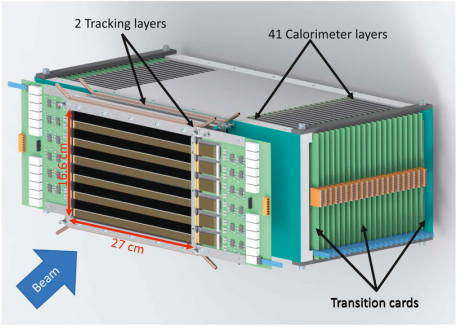

The track calorimeter consists of layers of pixel detectors and aluminium absorbers.

Schematic view of conception of a SPbU Digital tracking calorimeter.

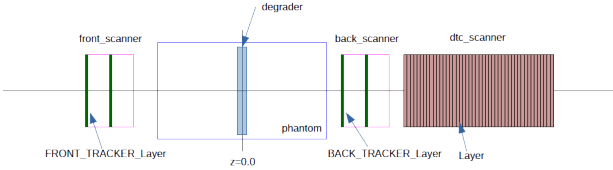

- Additional tracker (front scanner) in front of the patient.
- Optimisation of geometrical and material parameters.

Digital tracking calorimetry

Lasagne - like structure:

Schematic view of conception of a SPbU Digital tracking calorimeter.

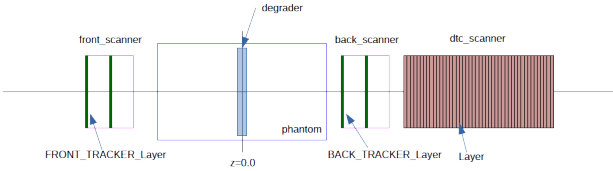

- Additional tracker (front scanner) in front of the patient.
- Optimisation of geometrical and material parameters.

Silicon pixel sensors

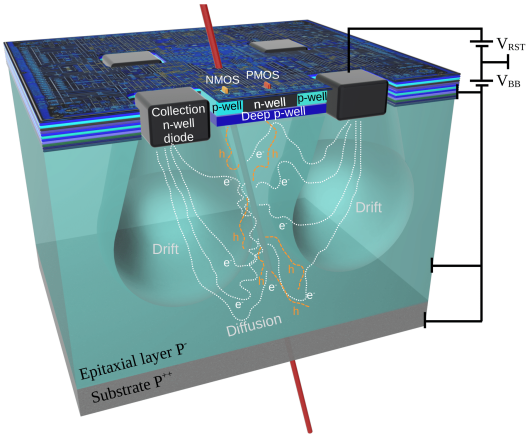

Structure of a pixel detector.

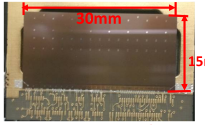

512 × 1024 sensitive pixels

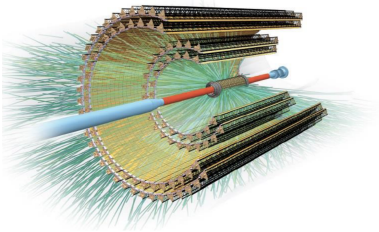

ALICE Inner Tracking System (Run 3)

B Abelev et al and (The ALICE Collaboration) 2014 J. Phys. G: Nucl. Part. Phys. 41 087002.

Layer structure of the digital tracker calorimeter

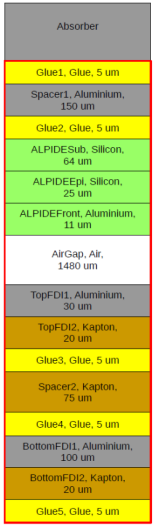

Absorber

Detecting layer 2000 um

Bergen pCT collaboration: 3.5 mm aluminium absorber in each layer.

J. Alme et al, Front. Phys. Sec. Med. Phys. and Imag. 2020; 8, 20

Layer structure of the digital tracker calorimeter

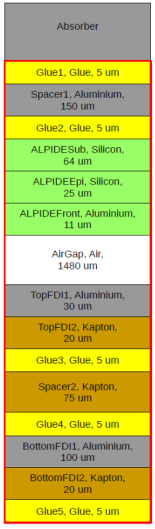

Absorber

Detecting layer 2000 um

Bergen pCT collaboration: 3.5 mm aluminium absorber in each layer.

J. Alme et al, Front. Phys. Sec. Med. Phys. and Imag. 2020; 8, 20

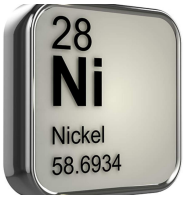

Advantages of nickel absorbers:

- Higher electron density leads leads to a reduction in proton ranges and a decrease in the number of layers.
- Low probability of production of unstable isotopes.

Monte-Carlo simulations of proton transport

Simulations were carried out within the GATE (Geant4 Application for Emission Tomography) software package.

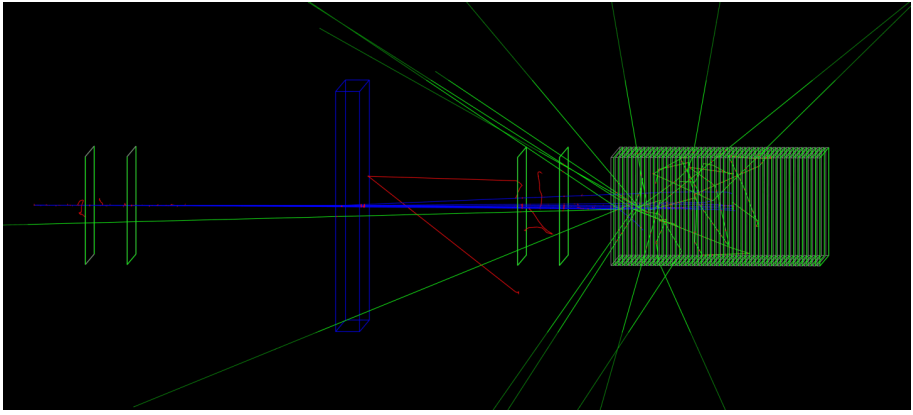

Each simulation included a transport of 20000 protons with initial energy 200 MeV through phantom area, tracking sensors and 45 layers of detectors and absorbers in calorimeter.

Resolution of System with *Al* absorbers

Al 3.5 mm:

Studying the distribution of the last layers for proton range.

Phantom	$\langle N \rangle$	σ	$\sigma/\langle N \rangle$
Water	26.1	0.46	0.0178
Air	29.7	0.53	0.0177

$$(\Delta\langle N \rangle = 3.6) > 5\sigma$$

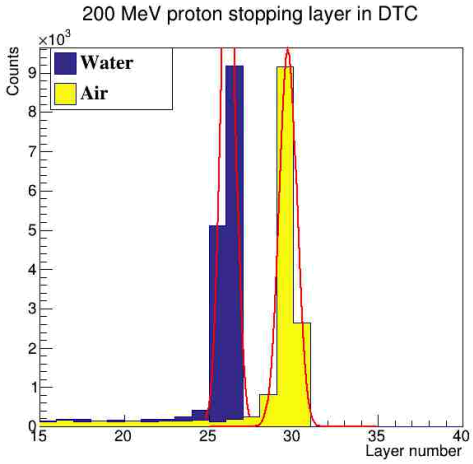

Clear separation of path distributions with a relative resolution of 1.7%

Resolution of System with *Ni* absorbers

Ni 3.5 mm:

Studying the distribution of the last layers for proton range.

Phantom	$\langle N \rangle$	σ	$\sigma/\langle N \rangle$
Water	8.8	0.5	0.030
Air	10.3	0.3	0.056

$$(\Delta\langle N \rangle = 1.5) < 3\sigma$$

Relative resolution is worse than for *Al*.
Overlapping path distributions.

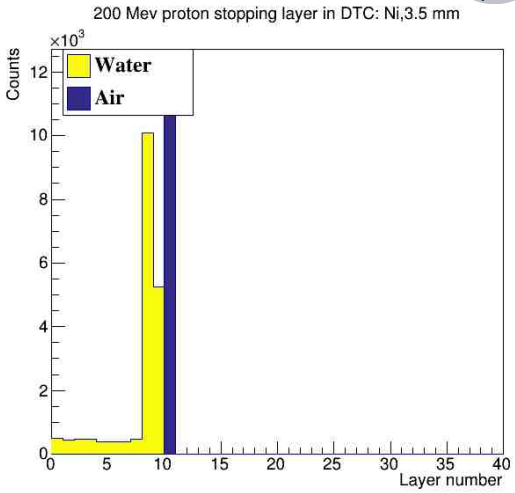

Resolution of System with *Ni* absorbers

Resolution ($\sigma/\langle N \rangle$) in dependence of *Ni* absorber thickness:

Water:

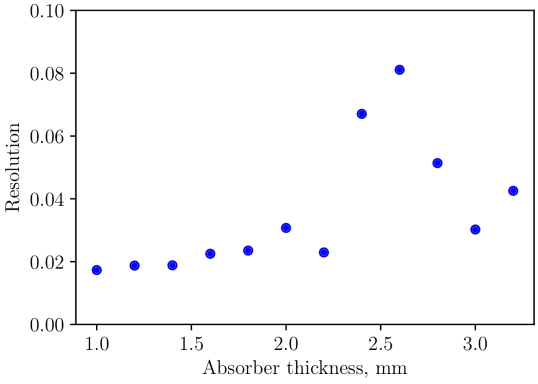

Air:

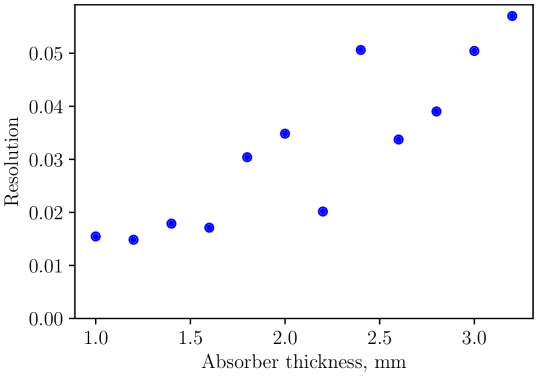

Resolution of System with *Ni* absorbers

Ni 1.5 mm:

Studying the distribution of the last layers for proton range.

Phantom	$\langle N \rangle$	σ	$\sigma/\langle N \rangle$
Water	20.1	0.4	0.017
Air	23.8	0.4	0.016

$$(\Delta\langle N \rangle = 3.7) > 5\sigma$$

- Relative resolution of 1.7% and clear separation of path distributions as for *Al* 3.5 mm.
- 22 layers for *Ni* vs 48 (Bergen pCT conception) layers for *Al*.

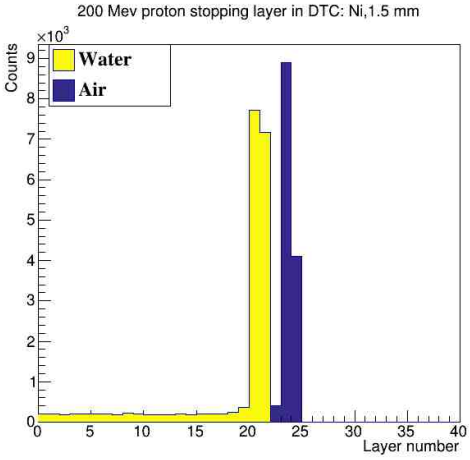

Economy of 2340 pixel chips!!!

Track finding ability

Track finding algorithm via Cellular Automaton:

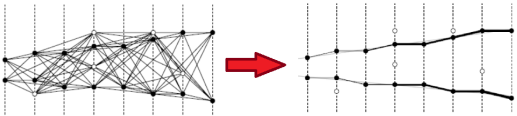

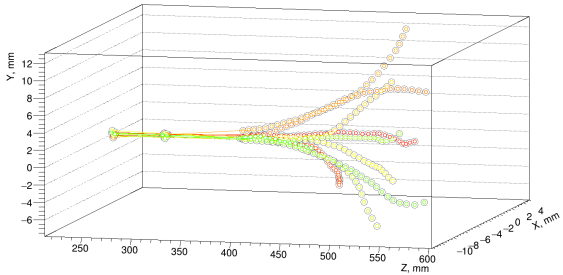

Reconstruction of 10 tracks in calorimeter with *Al* 3.5 mm absorbers.

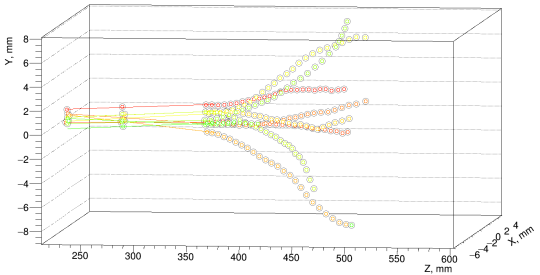

Reconstruction of 10 tracks in calorimeter with *Ni* 1.5 mm absorbers.

Track finding ability

Estimation of tracking quality as

$$\textit{Match rate} = \frac{\textit{Correctly identified hits}}{\textit{All hits}}.$$

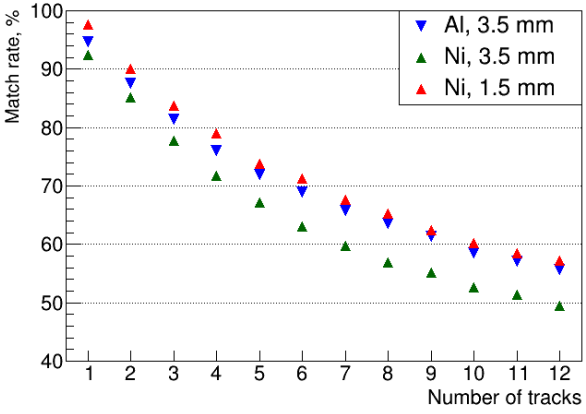

- Tracks recognition with multiple number of tracks at the same level for the model with *Ni* 1.5 mm and for *Al* 3.5 mm.
- Tracking quality for several tracks higher for *Ni* 1.5 mm absorbers.

Conclusions

The geometrical and material parameters were optimised in modelling simulations.

- Nickel absorbers provide provide a reduction in the number of layers and, as a consequence, the number detectors.
- Track reconstruction ability is higher with *Ni* absorbers.

Future plans include calculations with *Cu* absorbers (expected best thermal conductivity). Also simulations of silicon pixel sensors responses for more realistic track reconstruction is in development.

Thanks for the attention!